LBNL-49934
Preprint

ERNEST ORLANDO LAWRENCE
BERKELEY NATIONAL LABORATORY

Source-Independent Full Waveform Inversion of Seismic Data

Ki Ha Lee and Hee Joon Kim
Earth Sciences Division

March 2002
Submitted to
Geophysics

DISCLAIMER

DISCLAIMER

LBNL-49934

Source-Independent Full Waveform Inversion of Seismic Data

Ki Ha Lee and Hee Joon Kim

Earth Sciences Division
Ernest Orlando Lawrence Berkeley National Laboratory
University of California
Berkeley, California 94720

March 2002

This work was supported by the Director, Office of Science, Office of Basic Energy Sciences, of the U.S. Department of Energy under Contract No. DE-AC03-76SF00098, and by the Korea Science and Engineering Foundation (R01-2001-000071-0).

Source-independent full waveform inversion of seismic data

Ki Ha Lee * and Hee Joon Kim**

ABSTRACT

A rigorous full waveform inversion of seismic data has been a challenging subject primarily because of the lack of precise knowledge of the source. Conventional approaches involve some form of approximations to the source, so the inversion results are bound to be subject to the quality involved in the source approximation. The full waveform inversion methodology proposed and demonstrated in this paper does not require source information, therefore, the potential error involved in source estimation is eliminated. Seismic trace is first Fourier transformed in its entirety into the frequency domain and transfer functions are obtained. The transfer function is dimensionless, normalized frequency response and is complex. Normalization is done with any one data at arbitrary position among the data set. The transfer function is then shown to be uniquely defined as the normalized impulse response provided that a certain condition is met for the source. It is this property that allows construction of the proposed inversion algorithm without the source information. The algorithm minimizes misfits between data transfer function and the model transfer function. The methodology is applicable to any 3-D seismic problems, and damping can be easily included in the process. A proof of concept of the proposed approach has been successfully demonstrated using a simple 2-D scalar problem.

INTRODUCTION

It is common practice in seismic industry that the velocity structure is estimated by analyzing the traveltime of the seismic signal. In crosshole and surface-to-borehole applications, typical approach involves ray tracing in which the ray may be straight or curved depending on the degree of resolution desired, and more recently the Fresnel volume approach. The traveltime approach is fundamentally of high-frequency approximation with its maximum resolution on the order of a wavelength (Sheng and Schuster, 2000), or a fraction (5%) of the well separation in some practical cases. Furthermore, the usefulness of the result obtained from the ray tomography may be limited if the objective is to better understand the petrolophysical and hydrological 'properties' of the soil and rock; an increasingly important subject in characterizing petroleum and geothermal reservoirs and the environmental application of varying scales.

A better alternative to the traveltime approach appears to be the full waveform inversion. A number of recent studies on this subject (Sen and Stoffa, 1991; Kormendi and Dietrich, 1991; Minkoff and Symes, 1997; Zhou et al, 1997; Plessix and Bork, 1998; Pratt, 1999-a, 1999-b, to list a few) suggests that the full waveform inversion may provide improved resolution of the velocity and density structures. Furthermore, the amplitude and

* Ernest O. Lawrence Berkeley National Laboratory, MS 90-1116, Berkeley, California 94720. E-mail: KHLee@lbl.gov

** Pukyung National University, Department of Exploration Engineering, 599-1 Daeyoun-dong, Nam-ku, Pusan 608-737, Korea. E-mail: hejkim@pknu.ac.kr.

the phase of the waveform are, together, sensitive to the intrinsic energy loss of the propagating wave through dispersion, and to the petrophysical property of the material through which the wave propagates. Therefore, the full waveform analysis seems to be an attractive tool in investigating hydrological and petrophysical properties of the medium. To get to the full waveform inversion, however, there is one major difficulty to overcome. In all field applications, the effective source waveform and the coupling of the medium with the source and the receiver are not very well understood. The problem can be resolved to some extent with a good velocity approximation (Pratt, 1999-a), but in general, the measured signal cannot be properly calibrated, rendering the full waveform inversion a technical challenge.

In this paper we propose and describe a methodology to overcome this difficulty using the 'transfer function' approach. The transfer function described in the next section is completely independent of the actual source function, and it is this unique property that makes the proposed approach feasible. The proposed method allows the full waveform inversion without the knowledge of the transmitted waveform. If and when one desires to know the actual source function, the proposed method provides a deterministic means to reconstruct the source function once the inversion is carried out successfully.

TRANSFER FUNCTION

Without loss of generality, let us assume a field survey involving *NT* transmitter positions and *NG* receiver positions of arbitrary configurations. In acquiring data, configuration of source and receiver deployment is important part of survey design for successfully achieving the desired objective of the survey. The proposed full waveform inversion scheme is general in that any arbitrary configuration is acceptable; surface or single borehole reflection, surface-to-borehole or borehole-to-surface (VSP), or crosshole. In developing an inversion scheme for full 3-D problems using the transfer function, we require a full tensor measurement; three component measurements at each receiver position for each one of three transmitting events at each source position. The data may be in the form of pressure, displacement, velocity or acceleration, and may be described in general as

$$\boldsymbol{D}^d_{ji}(t) = \boldsymbol{S}_i(t) \otimes \boldsymbol{P}^d_{ji}(t) \otimes \boldsymbol{R}_j(t), \quad (j = 1 \sim NG;\ \ i = 1 \sim NT). \tag{1}$$

The superscript *d* indicates data and each constituent in this equation is a (3×3) tensor. It simply states that the data $\boldsymbol{D}^d_{ji}(t)$ recorded at the *j*-th receiver position are multiple convolution of the actually transmitted source $\boldsymbol{S}_i(t)$ that includes source system function and the radiation pattern caused by source-medium coupling, the impulse response $\boldsymbol{P}^d_{ji}(t)$ of the medium at the *j*-th receiver due to the *i*-th source, and the receiver system function $\boldsymbol{R}_j(t)$ including the medium-receiver coupling. In the following analysis we will drop $\boldsymbol{R}_j(t)$ assuming that receiver (geophone) calibration is known and the effect of medium-receiver coupling to data is relatively minor compared to that of the source waveform. The source function $\boldsymbol{S}_i(t)$ is in general not well understood, and this is an ongoing research by itself in order to improve the quality of data interpretation. The impulse response $\boldsymbol{P}^d_{ji}(t)$ is the solution to the governing differential equation with an impulse source in time at the *i*-th position. If we Fourier transform equation (1), $FT\{(D,S,P)(t)\} \rightarrow (\mathbf{D},\mathbf{S},\mathbf{P})(\omega)$, with the $R_j(t)$ term neglected, we get

$$\mathbf{D}^d_{ji}(\omega) = \mathbf{S}_i(\omega)\mathbf{P}^d_{ji}(\omega). \qquad (2)$$

The data in the frequency domain contains all information the time series has. Longitudinal and transverse waves of primary arrivals followed by events of converted modes, multiple reflections, and all other scattering waves caused by heterogeneities. Equation (2) simply states that data is the impulse response of the medium weighted by the source spectrum. In describing elements of individual tensors, let l = (1, 2, 3) define field components in Cartesian coordinate and k = (a, b, c) define three source events. We next assume that each event of k = (a, b, c) in turn consists of three unknown Cartesian components. The data at the j-th receiver position, equation (2), may then be described as

$$\mathbf{D}^d_{ji}(\omega) = \left\{\mathbf{d}^d_{aji}, \mathbf{d}^d_{bji}, \mathbf{d}^d_{cji}\right\}(\omega) = \begin{bmatrix} d^d_{1aji} & d^d_{1bji} & d^d_{1cji} \\ d^d_{2aji} & d^d_{2bji} & d^d_{2cji} \\ d^d_{3aji} & d^d_{3bji} & d^d_{3cji} \end{bmatrix}(\omega), \qquad (3)$$

due to the sources (three events k = a, b, and c) at the i-th position

$$\mathbf{S}_i(\omega) = \left\{\mathbf{s}_{ai}, \mathbf{s}_{bi}, \mathbf{s}_{ci}\right\}(\omega) = \begin{bmatrix} s_{1ai} & s_{1bi} & s_{1ci} \\ s_{2ai} & s_{2bi} & s_{2ci} \\ s_{3ai} & s_{3bi} & s_{3ci} \end{bmatrix}(\omega). \qquad (4)$$

Notice that if the events are made to align closely to the Cartesian components, the source matrix will be diagonally dominant. The tensor impulse response of the medium relating the diagonal impulse source at the i-th transmitter position to the measurements at the j-th receiver position may be written as

$$\mathbf{P}^d_{ji}(\omega) = \left\{\mathbf{p}^d_{1ji}, \mathbf{p}^d_{2ji}, \mathbf{p}^d_{3ji}\right\}(\omega) = \begin{bmatrix} p^d_{11ji} & p^d_{12ji} & p^d_{13ji} \\ p^d_{21ji} & p^d_{22ji} & p^d_{23ji} \\ p^d_{31ji} & p^d_{32ji} & p^d_{33ji} \end{bmatrix}(\omega). \qquad (5)$$

In defining the data transfer function, we first select the reference point, say j = 1. The tensor data transfer function is now defined by the data at $j = 1 \sim NG$, normalized by that of the reference point

$$\mathbf{T}_{ji}^{d}(\omega)=\frac{\mathbf{D}_{ji}^{d}(\omega)}{\mathbf{D}_{1i}^{d}(\omega)}=\frac{\mathbf{S}_{i}(\omega)\mathbf{P}_{ji}^{d}(\omega)}{\mathbf{S}_{i}(\omega)\mathbf{P}_{1i}^{d}(\omega)}$$

$$,\qquad (6)$$

$$=\mathbf{P}_{1i}^{d^{-1}}(\omega)\mathbf{P}_{ji}^{d}(\omega)=\begin{bmatrix} t_{11ji}^{d} & t_{12ji}^{d} & t_{13ji}^{d} \\ t_{21ji}^{d} & t_{22ji}^{d} & t_{23ji}^{d} \\ t_{31ji}^{d} & t_{32ji}^{d} & t_{33ji}^{d} \end{bmatrix}(\omega)$$

where the convention of the subscripts for the transfer function is the same as that used for impulse response. In equation (6) the source term cancels out itself, so the transfer function is defined as the normalized impulse response of the medium; hence the uniqueness of the transfer function. The necessary condition for the source term to cancel out is that the determinant of the source matrix is non-zero. In other words, three source events need to be linearly independent. This condition can be met, in principle, even if source events consist of explosions as long as their Cartesian constituents are linearly independent.

In this procedure we assume that for each source, $i = 1\sim NT$, NG measurements are made simultaneously. If for some reason all NG data cannot be taken simultaneously, a simultaneous data set may be simulated if neighboring subsets share at least one overlapping receiver position. Since we do not know the medium, the impulse response itself is not known either at this point.

FULL WAVEFORM INVERSION USING TRANSFER FUNCTION

To obtain the numerical solution for the impulse response for scalar and elastic wave equations one needs to spatially discretize the constitutive parameters, and apply finite difference, finite element, or integral equation technique to solve the discretized system. Using the finite difference or finite element method, the assembled system of equations, including the damping, takes a general form (Marfurt, 1984)

$$\mathbf{M}\ddot{p}(t)+\mathbf{C}\dot{p}(t)+\mathbf{K}p(t)=\mathbf{g}\delta(t), \qquad (7)$$

where the field vector $p(t)$ is the discretized wavefield, $\mathbf{M}$ is the mass matrix, $\mathbf{K}$ is the stiffness matrix, and $\mathbf{C}$ is the damping matrix. If there is a total of N unknowns in the distretization, all $\mathbf{M}$, $\mathbf{C}$, and $\mathbf{K}$ are $N\times N$ square matrices, the field vector $\boldsymbol{p}$ is $N\times 1$, and the load vector $\mathbf{g}$ is also $N\times 1$ whose entries are all zero except for 1s at the source locations. Boundary condition is included implicitly.

The reduced system of equations may be solved in the time domain, typically using the coupled first-order differential equations on a staggered grid (Virieux, 1984 and 1986; Levander, 1988; Randall, 1989; Yomogida and Etgen, 1993; Graves, 1996), or in the frequency domain (Pratt, 1990; Pratt and Worthington, 1990; Song and Williamson, 1995; Song et al., 1995; Pratt et al., 1998) after Fourier transforming equation (7), $FT\{p(t)\}\rightarrow\mathbf{p}(\omega)$, into

$$-\omega^{2}\mathbf{M}\mathbf{p}(\omega)+i\omega\mathbf{C}\mathbf{p}(\omega)+\mathbf{K}\mathbf{p}(\omega)=\mathbf{g}. \qquad (8)$$

Next, we will show that the transfer function defined by equation (6) is all that's needed for the full waveform inversion. In the inversion the objective functional typically consists of data misfit, and the misfit in transfer function can be used just for that purpose. For a given model one can generate synthetic data using equation (8), and then obtain the model transfer function similar to the data transfer function described by equation (6). Formally, the synthetic impulse response at the j-th receiver due to the i-th source may be obtained and designated as $\mathbf{P}_{ji}^{m}(\omega)$,

$$\mathbf{P}_{ji}^{m}(\omega)=\begin{bmatrix} p_{11ji}^{m} & p_{12ji}^{m} & p_{13ji}^{m} \\ p_{21ji}^{m} & p_{22ji}^{m} & p_{23ji}^{m} \\ p_{31ji}^{m} & p_{32ji}^{m} & p_{33ji}^{m} \end{bmatrix}(\omega). \tag{9}$$

where the superscript m indicates model. Accordingly, the model transfer function is obtained from the numerical solution for the given velocity model

$$\mathbf{T}_{ji}^{m}(\omega)=\mathbf{P}_{1i}^{m^{-1}}(\omega)\mathbf{P}_{ji}^{m}(\omega)=\begin{bmatrix} t_{11ji}^{m} & t_{12ji}^{m} & t_{13ji}^{m} \\ t_{21ji}^{m} & t_{22ji}^{m} & t_{23ji}^{m} \\ t_{31ji}^{m} & t_{32ji}^{m} & t_{33ji}^{m} \end{bmatrix}(\omega). \tag{10}$$

The inversion procedure starts with the misfit, with the subscripts to the transfer functions dropped

$$\phi(m)=\left\|\mathbf{W}_d\left(\mathbf{T}^m-\mathbf{T}^d\right)\right\|^2. \tag{11}$$

The misfit between data and model transfer functions at the reference point is always zero $\left(t_{lk1i}^{m}-t_{lk1i}^{d}=0.0\right)$. In setting up the data misfit real and imaginary parts are separated, so the actual number of data used for the inversion is $NEQ = 2{\times}NFREQ{\times}NT{\times}(NG-1){\times}9$, and the computation is done in real arithmetic. The variable $NFREQ$ is the total number of frequencies. The matrix $\mathbf{W}_d$ is an $NEQ{\times}NEQ$ weighting matrix representing the relative importance of each data.

For inversion we consider Gauss-Newton method by first expanding the objective functional, equation (11), into a Taylor series (Bertsekas, 1982; Tarantola, 1987; Oldenburg *et al.*, 1993; to list a few)

$$\phi(m+\delta m)=\phi(m)+\gamma_m{}^T\delta m+0.5\delta m^T\mathbf{H}_m\delta m+O\left\{(\delta m)^3\right\}. \tag{12}$$

Here, γ_m is an $M{\times}1$ column matrix consisting of elements $\left\{\frac{\partial\phi}{\partial m_p},\ p=1\sim M\right\}$ with M being the total number of parameters to be determined, and is compactly written as

$$\gamma_m = 2\mathbf{J}^T\mathbf{W}_d{}^T\mathbf{W}_d\left(\mathbf{T}^m - \mathbf{T}^d\right),$$

and $\mathbf{H}_m$ is an $M \times M$ square matrix (weighted and constrained Hessian) consisting of elements $\left\{\frac{\partial^2\phi}{\partial m_q \partial m_p},\ p,q=1 \sim M\right\}$ written as

$$\mathbf{H}_m = 2\mathbf{J}^T\mathbf{W}_d{}^T\mathbf{W}_d\mathbf{J} + O\left(\frac{\partial J}{\partial m}\right).$$

The last term is literally interpreted as the changes in the partial derivative of data (transfer function in this case) due to changes in the velocity. This term is small if either the residuals are small, or the forward differential equation is quasi linear (Tarantola, 1987). Furthermore, it is usually difficult to compute, so is generally dropped. For each frequency and source the sensitivity function (Jacobian) **J** is a $\{2 \times (NG\text{-}1) \times 9\} \times M$ rectangular matrix; $\{2 \times (NG\text{-}1) \times 9\}$ because real and imaginary parts have been separated for each of 9 tensor elements. For example, for the *i*-th source and a fixed frequency, the entries to the Jacobian corresponding to the *j*-th receiver and the *p*-th parameter may be obtained as

$$\begin{pmatrix} J_{p,l,k,(2*j-1),i} \\ J_{p,l,k,(2*j),i} \end{pmatrix} = \begin{pmatrix} \text{real} \\ \text{imaginary} \end{pmatrix} \frac{\partial}{\partial m_p} t^m_{lkji}; \quad l,k = 1,2,3\ , \tag{13}$$

with

$$\frac{\partial}{\partial m_p} t^m_{lkji} = \frac{\partial}{\partial m_p} \frac{p^m_{lkji}}{p^m_{lk1i}} = \frac{1}{p^m_{lk1i}} \left(\frac{\partial p^m_{lkji}}{\partial m_p} - \frac{p^m_{lkji}}{p^m_{lk1i}} \frac{\partial p^m_{lk1i}}{\partial m_p} \right); \quad i = 1 \sim NT; \quad j = 2 \sim NG; \quad p = 1 \sim M\ .$$

Evaluation of the partial derivatives of transfer function is straightforward because it only requires the partial derivatives of the model impulse response, which in turn may be obtained from the forward model results using equation (8). This feature is the essence of this paper; a rigorous full waveform inversion of seismic data can be done, and it does not require the knowledge of the actual source waveform. The partial derivatives with respect to model parameters can be efficiently evaluated, but will not be discussed here because the subject is beyond the scope of this paper.

The functional that will be minimized consists of the misfit, equation (12), and a constraint that will have a smoothing effect on the variation of the model in the updating process. Specifically, it may be written

$$\Phi(m + \delta m) = \phi(m + \delta m) + \lambda \|\mathbf{W}_m \delta m\|^2, \tag{14}$$

where λ is the Lagrange multiplier that controls relative importance of data misfit and the behavior of the parameter variation, and $\mathbf{W}_m$ an $M \times M$ controlling matrix. When the matrix is diagonal it has an effect of keeping the parameter from changing from the current one. On the other hand, if the matrix represents a gradient operator its effect is to spatially smooth out the changes. Minimization of functional (14) with respect to perturbation in model parameter results in a system of normal equations

$$\left(\mathbf{J}^T\mathbf{W}_d{}^T\mathbf{W}_d\mathbf{J}+\lambda\mathbf{W}_m{}^T\mathbf{W}_m\right)\delta m=-\mathbf{J}^T\mathbf{W}_d{}^T\mathbf{W}_d\left(\mathbf{T}^m-\mathbf{T}^d\right), \tag{15}$$

from which the model parameter at the (k+1)-th iteration is updated to

$$m^{k+1}=m^k+\delta m.$$

The iteration stops when the change in parameter is below a preset tolerance, typically given in terms of root mean square (rms).

CONSTRUCTION OF SOURCE FUNCTION

Once the inversion is successful, the functional description of the actual source waveform can be established using deconvolution. Specifically, the deconvolution can be achieved by dividing the data with the impulse response of the synthetic model that has been obtained through the inversion process. From equation (2), the deconvolution tensor may be estimated to be

$$\mathbf{C}_{ji}(\omega)=\mathbf{P}_{ji}^{m^{-1}}(\omega)\mathbf{D}_{ji}^{d}(\omega)=\begin{bmatrix} c_{1aji} & c_{1bji} & c_{1cji} \\ c_{2aji} & c_{2bji} & c_{2cji} \\ c_{3aji} & c_{3bji} & c_{3cji} \end{bmatrix}(\omega). \tag{16}$$

Notice that the elements of the impulse response of the model $\mathbf{P}_{ji}^{m}(\omega)$ are independent of the source events (a, b, c), but the elements of the deconvolution tensor $\mathbf{C}_{ji}(\omega)$ are related to the source events. If the data and the inversion process were exact, the deconvolution function $\mathbf{C}_{ji}(\omega)$ is actually the frequency spectrum of the source, and it must be identical for all receiver position. Since neither the data nor the inversion process is exact, the source function may be obtained by taking a statistical mean of the deconvolution function at different receiver positions. For example the first element of the source function in equation (4) may be estimated using the root mean square approach

$$\mathbf{s}_{1ai}(\omega)=\sqrt{\frac{1}{NG}\sum_{j=1}^{NG}\left\{c_{1aji}(\omega)\right\}^2}. \tag{17}$$

Since the function $\mathbf{C}_{ji}(\omega)$ itself is complex the averaging process has to be in amplitude and phase, or real and imaginary parts, separately. Inverse Fourier transforming, $FT^{-1}\{\mathbf{S}_i(\omega)\}\rightarrow S_i(t)$, one obtains the source function in time

$$S_i(t)=\left\{s_{ai},s_{bi},s_{ci}\right\}(t)=\begin{bmatrix} s_{1ai} & s_{1bi} & s_{1ci} \\ s_{2ai} & s_{2bi} & s_{2ci} \\ s_{3ai} & s_{3bi} & s_{3ci} \end{bmatrix}(t). \tag{18}$$

Note that each one of three events (a,b,c), for example $s_{ai}(t) = \{s_{1ai}, s_{2ai}, s_{3ai}\}^T(t)$, will produce complete description of the source at the transmitter location i as a function of time. The function $S_i(t)$ describes the source at the i-th transmitter position that would most likely have produced data $D_{ji}^d(t)$, $j = 1 \sim NG$, shown in equation (1). The reconstructed source function is the effective source at the time of the event and it will include spatial and temporal radiation patterns as well.

FULL WAVEFORM INVERSION OF 2-D ACOUSTIC VELOCITY

The proposed inversion scheme has been tested using a simple 2-D acoustic model. Let us consider the impulse response governed by a 2-D acoustic wave equation in the frequency domain

$$\nabla^2 p(x_r, x_s, \omega) + \frac{\omega^2}{v^2} p(x_r, x_s, \omega) + \delta^2(x - x_s) = 0, \tag{19}$$

where the impulse response p is the scalar pressure wavefield, v the velocity, and (x_r, x_s) receiver and source positions. The source is a 2-D Kronecker's delta function in space, and is also a delta function at $t = 0$ in the time-domain formulation. A finite-element modeling (FEM) scheme is used to generate the synthetic impulse response. The model parameter is the acoustic velocity in each of the rectangular elements used for the FEM solution. Following the procedure described in the previous section, the scalar synthetic transfer function is obtained from the numerical solution for the given velocity model

$$t_{ji}^m(\omega) = \frac{p_{ji}^m(\omega)}{p_{1i}^m(\omega)}, \quad (j = 1 \sim NG; \ \ i = 1 \sim NT), \tag{20}$$

The inversion procedure starts with an objective functional, equation (14), reduced to handle scalar problem. The number of equation is $NEQ = 2 \times NFREQ \times NT \times (NG - 1)$, and the computation is done in real arithmetic. Related sensitivity functions are

$$\begin{pmatrix} J_{p,(2*j-1),i} \\ J_{p,(2*j),i} \end{pmatrix} = \begin{pmatrix} \text{real} \\ \text{imaginary} \end{pmatrix} \frac{\partial}{\partial m_p} t_{ji}^m ,$$

with

$$\frac{\partial}{\partial m_p} t_{ji}^m = \frac{\partial}{\partial m_p} \frac{p_{ji}^m}{p_{1i}^m} = \frac{1}{p_{1i}^m} \left(\frac{\partial p_{ji}^m}{\partial m_p} - \frac{p_{ji}^m}{p_{1i}^m} \frac{\partial p_{1i}^m}{\partial m_p} \right); \ \ i = 1 \sim NT; \ \ j = 2 \sim NG; \ \ p = 1 \sim M .$$

The model used for the test is a broken dipping fault in a background of 3000 m/s constant velocity. The fault consists of a 6 m thick low velocity (2500 m/s) layer overlain by another 6 m thick high velocity (3500 m/s) layer. A crosshole configuration is used for the exercise, with the borehole at x = - 45 m for the transmitter (Tx) borehole and the other at x = 45 m for the receiver (Rx) borehole. A total of 21 line sources are used with an equal vertical separation of 9 m, and same number of receivers and separation for the receivers. For each source pressure wavefields computed at 21 receiver positions have been normalized by the first pressure wavefield, resulting in 21 transfer functions. The number of frequencies used is 10; starting from 10 Hz to 100 Hz, linearly separated by 10 Hz. The shortest wavelength in the background is 30 m, so the maximum resolution is expected to be on the order of 7 to 8 m if we take into account of the wavelength as a measure of resolution. Using the numerical solution of the model as synthetic data, the inversion was started with an initial model of 2850 m/s uniform whole space. A grid of uniform cell size, 3 m by 3 m, has been used throughout. The inversion domain is 120 m by 180 m, containing a total of 2400 velocity parameters.

The size of the matrix from equation (15) is relatively modest for the test model, so we solved it using QR decomposition with successive Householder transformations. The Lagrange multiplier λ is automatically selected in the inversion process. It starts with executing a given number, say *nl*, of inversions using *nl* different multipliers that are spaced appropriately. The same Jacobian is used at this step. As a result *nl* updated parameter sets are produced, followed by *nl* forward model calculations resulting in *nl* data misfits. Among these, we choose the model and parameter λ giving the lowest data misfit.

To demonstrate the validity of the proposed inversion scheme, we first carried out conventional inversion using impulse response, and the result is shown in Figure 1b. By what we mean conventional, we assume that the source waveform is known, so data can be reduced to impulse response and inversion is carried out using the impulse response. Separate from this, we also obtained velocity structure using transfer function approach and the result is shown in Figure 1c. In this exercise we used $nl = 3$ in each iteration to select parameter update and Lagrange multiplier. After 5 iterations, two results appear almost identical. Slight difference may have been due to the fact that the transfer function approach has one less data than the impulse response approach because one data was used to normalize the others. The behaviors of the rms are similar too. Figure 2 shows the comparison in rms with impulse response and with transfer function. Note that the Lagrange multiplier also changes as iteration is continued. There is room for improvements in the quality of inversion by using higher frequency data and denser deployment of transmitters and receivers, but the main objective seems to have been achieved.

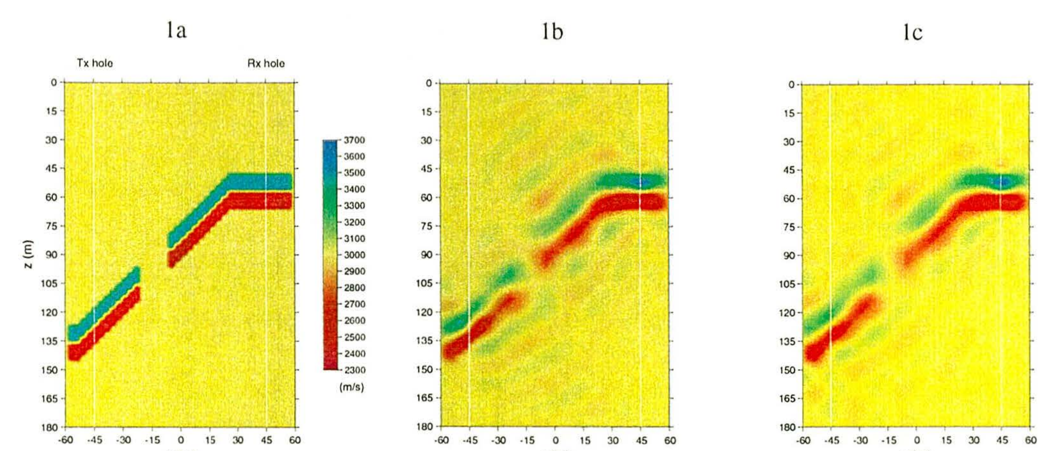

Fig. 1. Comparison of full waveform inversion results using a fault model in a background of 3000 m/s constant velocity: 1a) A 2-D velocity model. 1b) Inversion result using impulse response. 1c) Inversion result using transfer function.

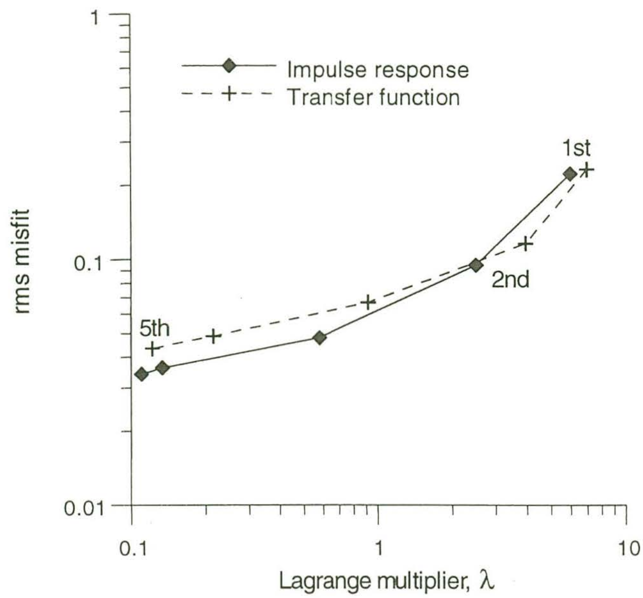

Fig. 2. Convergence in rms misfits and associated Lagrange multiplier as a function of iteration during the full waveform inversion.

CONCLUSIONS

An innovative, rigorous full waveform inversion scheme has been proposed and the validity of the scheme successfully demonstrated using a simple 2-D synthetic model. The highlight of the proposed scheme is that full waveform inversion of seismic data can be accomplished without the source information, taking advantage of the useful property of the transfer function. Under proper combination of sources and receivers the transfer function is shown to be uniquely determined in terms of the normalized impulse response. The methodology is easily extended to include general 3-D problems. As an important byproduct, it has also been shown that the source function can be reconstructed once the full waveform inversion is completed. The reconstructed source function describes the effective source, not the source system output, at the time of event, including spatial and temporal radiation patterns.

ACKNOWLEDGMENTS

This work was supported by the Office of Basic Energy Sciences, Engineering and Geosciences Division of the U.S. Department of Energy under Contract No. DE-AC03-76SF00098. The first author acknowledges the sabbatical leave granted by the Earth Sciences Division of the E. O. Lawrence Berkeley National Laboratory. The proposed idea was put into work during this period. Korea Science and Engineering Foundation (R01-2001-000071-0) provided support for the second author for his participating in this study.

REFERENCES

Bertsekas, D. P., 1982, Enlarging the region of convergence of Newton's method for constrained optimization, J. Optimization Theory Applications, **36**, 221-251.

Graves, R. W., 1996, Simulating seismic wave propagation in 3D elastic media using staggered-gris finite differences, Bull. Seism. Soc. Am., **86**, 1091-1106.

Kormendi, F., and Dietrich, M., 1991, Nonlinear waveform inversion of plane-wave seismograms in stratified elastic media, Geophysics, **56**, 664-674.

Levander, A. R., 1988, Fourth-order finite difference P-SV seismograms, Geophysics, **53**, 1425-1436.

Marfurt, K. J., 1984, Accuracy of finite-difference and finite-element modeling of the scalar and elastic wave equations, Geophysics, **49**, 533-549.

Minkoff, S. E., and Symes, W. W., 1997, Full waveform inversion of marine reflection data in the plane-wave domain, Geophysics, **62**, 540-553.

Oldenburg, D. W., McGillivray, P. R., and Ellis, R. G., 1993, Generalized subspace methods for large-scale inverse problems, Geophys. J. Int., **114**, 12-20.

Plessix, R.- E., and Bork, J., 1998, A full waveform inversion example in VTI media: 68th Ann. Internat. Mtg., Soc. Expl. Geophys., Expanded Abstracts, 1562-1565.

Pratt, R. C., 1990, Inverse theory applied to multi-source cross-hole tomography, Part II: elastic wave-equation method, Geophys. Prospect., **38**, 311-330.

Pratt, R. G., 1999-a, Seismic waveform inversion in frequency domain, Part 1: Theory and verification in physical scale model, Geophysics, **64**, 888-901.

——, 1999-b, Seismic waveform inversion in frequency domain, Part 2: Fault delineation in sediments using crosshole data, Geophysics, **64**, 902-914.

Pratt, R. G., Shin, C., Hicks, G. J., 1998, Gauss-Newton and full Newton methods in frequency-space seismic waveform inversion, Geophys. J. Int., **133**, 341-362.

Pratt, R. G., and Worthington, M. H., 1990, Inverse theory applied to multi-source cross-hole tomography, Part I: acoustic wave-equation method, Geophys. Prospect., **38**, 287-310.

Randall, C. J., 1989, Absorbing boundary condition for the elastic wave equation, velocity-stress formulation, Geophysics, **54**, 1141-1152.

Sen, M. K., and Stoffa, P. L., 1991, Nonlonear one-dimensional seismic waveform inversion using simulated annealing, Geophysics, **56**, 1624-1638.

Sheng, J., and Schuster, G. T., 2000, Finite-frequency resolution limits of traveltime tomography for smoothly varying velocity models: 70th Ann. Internat. Mtg., Soc. Expl. Geophys., Expanded Abstracts, 2134-2137.

Song, Z.- M., and Williamson, P. R., 1995, Frequency-domain acoustic modeling and inversion of crosshole data: part I-2.5-D modeling method, Geophysics, **60**, 784-795.

Song, Z.- M., Williamson, P. R., and Pratt, R. G., 1995, Frequency-domain acoustic wave modeling and inversion of crosshole data: Part II-inversion method, synthetic experiments and real-data results, Geophysics, **60**, 796-809.

Virieux, J., 1984, P-SV wave propagation in heterogeneous media: velocity-stress finite-difference method, Geophysics, **51**, 889-901.

Virieux, J., 1986, SH wave propagation in heterogeneous media: velocity-stress finite-difference method, Geophysics, **49**, 1933-1957.

Tarantola, A., 1987, Inverse Problem Theory: Methods for Data Fitting and Parameter Estimation: Elsevier, Amsterdam.

Yomogida, K., and Etgen, J. T., 1993, 3-D wave propagation in the Los Angeles Basin for the Whittier-Narrows earthquake, Bull. Seism. Soc. Am. **83**, 1325-1344.

Zhou, C., Schuster, G. T., Hassanzadeh, S., and Harris, J. M, 1997, Elastic wave equation traveltime and wavefield inversion of crosswell data, Geophysics, **62**, 853-868.

ERNEST ORLANDO LAWRENCE BERKELEY NATIONAL LABORATORY
ONE CYCLOTRON ROAD | BERKELEY, CALIFORNIA 94720

Prepared for the U.S. Department of Energy under Contract No. DE-AC03-76SF00098